International Journal of Modern Manufacturing Technologies
ISSN 2067–3604, Vol. X, No. 1 / 2018

STABILITY LOBES PREDICTION IN HIGH SPEED MILLING

Azoui Cherifa[1], Benbrahim Mohamed[2]

[1]Mechanical Engineering Department, Faculty of Technology, University of Batna 2, 01 Avenue Chahid Boukhlouf Mohamed El Hadi, Batna (05000), Algeria
[2]LRP (Production Research Laboratory), Mechanical Engineering Department, Faculty of Technology, University of Batna 2, 01 Avenue Chahid Boukhlouf Mohamed El Hadi, Batna (05000), Algeria

Corresponding author: Azoui Cherifa, az.cherifa@gmail.com

Abstract: Different techniques are used to obtain approximate solutions for delayed functional differential equations (RFDEs). All these models used the so-called stability lobe diagrams, to choose the maximum axial depth of cut for a given spindle speed associated with a free chatter in machining. In this research paper, the ZOA (Zeroth Order Approximation) and SD (Semi Discretization) methods are explained, developed and used to obtain the stability lobe diagrams for a milling cutting system with two degree of freedom, in high speed machining case.

Key words: high speed milling, vibrations, stability lobes, zeroth order approximation method (ZOA), semi discretization method (SD).

1. INTRODUCTION

Metal cutting processes could entail three different kinds of mechanical vibrations that arise due to the lack of dynamic stiffness of one or several elements of machining system composed by machine tool, tool holder, cutting tool and the work piece material. These kinds of vibrations are known as free, forced and self-excited vibrations, (Palpandian et al., 2013).

1.1 Free vibrations

When any external energy source is applied to initiate vibrations and is then removed, the consequential vibrations are known as free vibrations. In the absence of non-conservative forces, free vibrations sustain themselves and are periodic. The structure will vibrate in its natural mode until the damping causes the motion to die out.

1.2 Forced vibrations

Forced vibrations occur due to external harmonic excitations. The principle source of forced vibrations in milling processes is when the cutting edge enters and exits the machined piece. However, forced vibrations are also associated, with unbalanced bearings or cutting tools, or it could be transmitted by other machine tools through the workshop floor. Free and forced vibrations could be avoided or reduced if the causes of the vibration are identified. In this field, a variety of methods and techniques have been developed to mitigate and reduce their occurrence (Khaled et al, 2013).

1.3 Self-excited vibrations

Machine tool chatter is the self–excited relative oscillation between the cutting tool and work-piece that is developed under large metal remove rate. It is known that chatter occurs when there is a dynamic flexibility between the tool and the work piece, and when the magnitude of axial depth of cuts are larger than critical stability limits. It was shown that the border between a stable machining area (i.e. no chatter) and the unstable one (i.e. with chatter) could be visualized in terms of the axial depth of cut in a function of the spindle speed. These results are called stability lobe diagrams. By using these diagrams, it is possible to find the specific combination of machining parameters, which results in the maximum chatter-free material removal rate (Rubio et al 2004).

In order to avoid the consequences of self-excited vibrations, it is not often possible to use certain cutting systems, because they cause unstable operations of the used machine tools. Diagrams showing the stable and unstable areas of machine tools operations are called stability lobe diagrams (SLD), and they are defined according to the number of revolutions of the main spindle and the cutting depth. Stability lobe diagrams are usually defined analytically based on the modal parameters of the machining system and the parameters of the cutting process. The first research on mathematical modeling of self-excited vibrations were conducted by Tobias and Tlusty (Paurobally and Siddhpura, 2012), which identified a regenerative mechanism of self-excited

vibrations and developed a mathematical model in the form of delay differential equations (DDE). The proposed zeroth approximation (ZOA) method of Altintas and Budak (Altintas, and Budak ,1995), suggest to making stability predictions by using the zeroth order Fourier term, to approximate the cutting force variation and to achieve reasonably accurate stability lobe diagrams predictions for machining processes, for the less cutting force, i.e. for considerable radial immersions and large number of teeth. Besides to this, many researchers have also applied complicated mathematical expressions for modeling self-excited vibrations in order to define stability lobe diagrams. Insperger and Stephan (Insperger and Stépan, 2004) have applied the semi discretization method (SD) to reduce the complicated DDE method in terms of series of ordinary differential equations (ODE) with a known solution,(Mlađenović et al 2015). In this research paper the ZOA and SD methods are explained, developed, used and compared to obtain the stability lobe diagrams by using the Altintas studies (Altintas , 2000)and the Insperger and Stépan research work (Insperger and Stépan, 2004).

2. ZEROTH ORDER APPROXIMATION (ZOA) METHOD

Milling forces excite both cutter and work piece causing vibrations which are imprinted on the piece cutting surface. Each vibrating cutting tooth removes the wavy surface left from previous tooth, resulting in modulated chip thickness, Figure 1 (Wiercigroch and Budak, 2001).

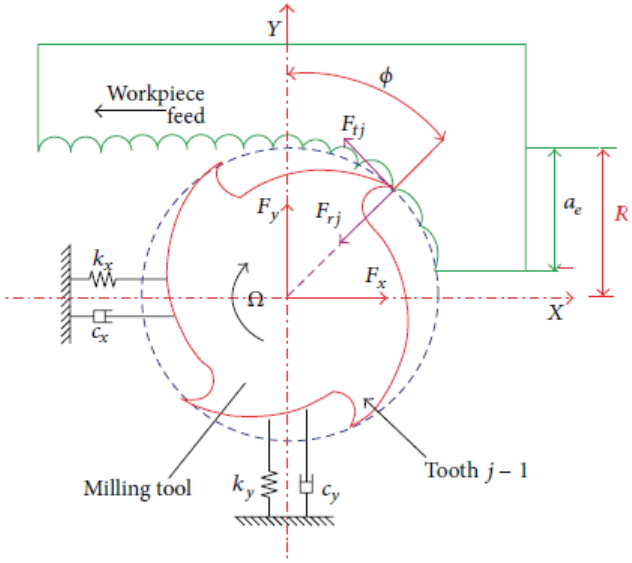

Fig. 1. Schematic mechanical model of two degrees of freedom milling system, (Jin et al, 2013).

The cutter used in the present study is assumed to be a system with one mode of vibration in each direction, X and Y, and the feed direction is along the X-axis. The milling system is shown in Figure 1, where the X-Y coordinates system is fixed with respect to the machine tool structure and its axes are aligned with the principal modes of oscillation. The milling cutter presents N teeth. They are assumed to be equally spaced. The cutting forces F_x and F_y are expressed as follows:

$$\begin{Bmatrix} F_x \\ F_y \end{Bmatrix} = \frac{1}{2} b k_t \begin{bmatrix} \alpha_{xx} & \alpha_{xy} \\ \alpha_{yx} & \alpha_{yy} \end{bmatrix} \begin{Bmatrix} \Delta x \\ \Delta y \end{Bmatrix} = \frac{1}{2} b k_t \left[A(t)\right]\{\Delta t\} \quad (1)$$

where the time–varying directional dynamic milling forces are given by the following expressions:

$$\alpha_{xx} = \sum_{j=0}^{N-1} -g_j \left[\sin 2\phi_j + K_r \left(1-\cos 2\phi_j\right)\right] \quad (2)$$

$$\alpha_{xy} = \sum_{j=0}^{N-1} -g_j \left[\left(1+\cos 2\phi_j\right) + K_r \sin 2\phi_j\right] \quad (3)$$

$$\alpha_{yx} = \sum_{j=0}^{N-1} g_j \left[\left(1-\cos 2\phi_j\right) - K_r \sin 2\phi_j\right] \quad (4)$$

$$\alpha_{yy} = \sum_{j=0}^{N-1} g_j \left[\sin 2\phi_j - K_r \left(1+\cos 2\phi_j\right)\right] \quad (5)$$

Considering that the angular position of the parameters changes with time and angular velocity, we could express equation (1) in time domain as a matrix form:

$$\{F(t)\} = \frac{1}{2} b K_t \left[A(t)\right]\{\Delta(t)\} \quad (6)$$

As the cutter rotates, the directional factors vary with time and this is the fundamental difference between milling process and other machining operations, such as turning where the force direction is constant. However, as for milling forces, [A(t)] is periodic at tooth passing frequency ($\omega_n=2\pi$) or tooth period ($T=2\pi/\omega_n$). Thus it could be expanded into a Fourier series:

$$\left[A(t)\right] = \sum_{r=-\infty}^{\infty} \left[A_r\right] e^{i r \omega_n t} \quad (7)$$

$$\left[A_r\right] = \frac{1}{T} \int_0^T \left[A(t)\right] e^{-i r \omega_n t} dt \quad (8)$$

The number of harmonics, r, of the tooth passing frequency, ω_n, is to be considered for an accurate reconstruction of [A(t)], and depends on the immersion conditions and on the number of teeth in cut. If the most simplistic approximation, the average component of the Fourier series expansion, is considered (i.e., r=0), then:

$$[A_0]=\frac{1}{T}\int_0^T[A(t)]dt \quad (9)$$

Since [A_0] is valid only between the cutter's entry (ϕ_{st}) and exit (ϕ_{ex}) angles, it becomes equal to the average value of [A(t)] at cutter pitch angle ($\phi_p=2\pi/N$) and its expression became:

$$[A(0)]=\frac{1}{\phi_p}\int_{\phi_{st}}^{\phi_{ex}}[A(\phi)]d\phi=\frac{N}{2\pi}\begin{bmatrix}\alpha_{xx} & \alpha_{xy}\\ \alpha_{yx} & \alpha_{yy}\end{bmatrix} \quad (10)$$

where the integrated functions are given as follows:

$$\alpha_{xx}=\frac{1}{2}\left[\cos 2\phi-2K_r\phi+K_r\sin 2\phi\right]_{\phi_{st}}^{\phi_{ex}} \quad (11)$$

$$\alpha_{xy}=\frac{1}{2}\left[-\sin 2\phi-2\phi+K_r\cos 2\phi\right]_{\phi_{st}}^{\phi_{ex}} \quad (12)$$

$$\alpha_{yx}=\frac{1}{2}\left[-\sin 2\phi+2\phi+K_r\cos 2\phi\right]_{\phi_{st}}^{\phi_{ex}} \quad (13)$$

$$\alpha_{yy}=\frac{1}{2}\left[-\cos 2\phi-2K_r\phi-K_r\sin 2\phi\right]_{\phi_{st}}^{\phi_{ex}} \quad (14)$$

The average directional factors depend on radial cutting constant, K_r, and on the width of cut bound by considering the entry (ϕ_{st}) and exit (ϕ_{ex}) angles. The dynamic milling expression (6) is then reduced to the following form:

$$\{F(t)\}=\frac{1}{2}b\,K_t\,[A_0]\{\Delta(t)\} \quad (15)$$

where [A_0] is the time invariant and the immersion depends on directional cutting matrix coefficient, , (Altintas, 2000).

Thus, the transfer function matrix at the cutter contact zone is given as follows:

$$[\phi(i\omega)]=\begin{pmatrix}\phi_{xx}(i\omega) & \phi_{xy}(i\omega)\\ \phi_{yx}(i\omega) & \phi_{yy}(i\omega)\end{pmatrix} \quad (16)$$

Furthermore, we describe the vibrations at the cutter frequency (ω_c) in the frequency domain by using harmonic functions:

$$\begin{aligned}\{r(i\omega_c)\}&=[\phi(i\omega)]\{f\}e^{i\omega_c t}\\ \{r_0(i\omega_c)\}&=e^{-i\omega_c T}\{r(i\omega_c)\}\\ \{\Delta r(i\omega_c)\}&=\{r(i\omega_c)\}-\{r_0(i\omega_c)\}\end{aligned} \quad (17)$$

The equation (15) could be written as:

$$\{F\}e^{i\omega_c t}=\frac{1}{2}bK_t\left[1-e^{-i\omega_c T}\right][A_0][\Phi(i\omega_c)]\{F\}e^{i\omega_c t} \quad (18)$$

The resulting characteristic equation becomes:

$$\det\left([I]+\Lambda\begin{bmatrix}\alpha_{xx} & \alpha_{xy}\\ \alpha_{yx} & \alpha_{yy}\end{bmatrix}\begin{bmatrix}G_x(i\omega_c) & 0\\ 0 & G_y(i\omega_c)\end{bmatrix}\right)=0 \quad (19)$$

$$with:\ \Lambda=-\frac{N}{4\pi}bK_t\left[1-e^{-i\omega_c t}\right] \quad (20)$$

Λ are the eigen values of the characteristic equation. For the case where the cross transfer functions of the system are neglected, its characteristic equation will be reduced to a quadratic equation form as:

$$a_0\Lambda^2+a_1\Lambda+1=0 \quad (21)$$

where:

$$a_0=G_x(i\omega_c)G_y(i\omega_c)\left(\alpha_{xx}\alpha_{yy}-\alpha_{xy}\alpha_{yy}\right) \quad (22)$$

$$a_1=\alpha_{xx}G_x(i\omega_c)+\alpha_{yy}G_y(i\omega_c) \quad (23)$$

Then, the eigen values Λ are obtained as follows, (Van Ballegooijen, 2008):

$$\Lambda=-\frac{1}{2a_0}\left(a_1\pm\sqrt{a_1^2-4a_0}\right) \quad (24)$$

The critical axial depth of cut could be obtained by substituting the Λ eigen values into equation (20):

$$b_{\lim}=-\frac{2\pi\Lambda_r}{N\,K_t}\left(1+K^2\right) \quad (25)$$

where: $K=\frac{\Lambda_i}{\Lambda_R}$ is obtained from equation (24).

Corresponding to the spindle speed, [7]:

$$\Omega=\frac{60}{NT} \quad (26)$$

The chatter frequency could be found as follows, (Altintas, 2000):

$$\begin{cases}\omega_c T=\varepsilon+2k\pi\\ \varepsilon=\pi-2\varphi\\ \varphi=\tan^{-1}K\end{cases} \quad (27)$$

where:

ε is the phase difference between the inner and outer modulations,

k is an integer corresponding to the number of vibration waves within a tooth period, Ω is the spindle speed (rpm), (Wiercigroch and Budak, 2001).

The transfer functions of the machine tool system are identified and the dynamic cutting coefficients are evaluated from the derived equation for a specified cutter and its radial immersion, from (Van Ballegooijen, 2008)

3. SEMI DISCRETIZATION (SD) METHOD

Semi discretization is a robust and powerful method to determine the structural behavior of linear delay differential equations (DDE's) in time domain. As a result of the constant delay, the present state could not identify the state of the DDE. This indicates that the past state: x(t − s), with $s \in [0,\tau]$ is necessary and an infinite dimensional function space is formulated. Semi discretization method could be used to perform the stability investigation of an existing steady state solution (for an autonomous system such as a turning process) or an existing periodic orbit (for a non-autonomous system such as a milling process),(Insperger and Stépan, 2004).
The governing equation of motion for a 2 DOF milling system with a symmetric tool is given by:

$$\begin{pmatrix}\ddot{x}(t)\\ \ddot{y}(t)\end{pmatrix}+\begin{pmatrix}2\zeta\omega_n & 0\\ 0 & 2\zeta\omega_n\end{pmatrix}\begin{pmatrix}\dot{x}(t)\\ \dot{y}(t)\end{pmatrix}+\begin{pmatrix}\omega_n^2+\frac{bh_{xx}(t)}{m_t} & \frac{bh_{xy}(t)}{m_t}\\ \frac{bh_{yx}(t)}{m_t} & \omega_n^2+\frac{bh_{yy}(t)}{m_t}\end{pmatrix}\begin{pmatrix}x(t)\\ y(t)\end{pmatrix}=\begin{pmatrix}\frac{bh_{xx}(t)}{m_t} & \frac{bh_{xy}(t)}{m_t}\\ \frac{bh_{yx}(t)}{m_r} & \frac{bh_{yy}(t)}{m_t}\end{pmatrix}\begin{pmatrix}x(t-\tau)\\ y(t-\tau)\end{pmatrix} \quad (28)$$

Where the angular natural frequency (ω_n), the relative damping (ζ) and the modal mass (m_t) of the tool are considered to be equal in both *x* and *y* directions, corresponding to the symmetric tool assumption. In equation (28), $h_{xx}(t)$, $h_{xy}(t)$, $h_{yx}(t)$ and $h_{yy}(t)$ are the four projections of the specific cutting force coefficients and they are defined as follows:

$$h_{xx}(t)=\sum_{j=1}^{N} g(\phi_j(t))\sin(\phi_j(t))\left(k_t\cos(\phi_j(t))+k_n\sin(\phi_j(t))\right) \quad (29)$$

$$h_{xy}(t)=\sum_{j=1}^{N} g(\phi_j(t))\cos(\phi_j(t))\left(k_t\cos(\phi_j(t))+k_n\sin(\phi_j(t))\right) \quad (30)$$

$$h_{yx}(t)=\sum_{j=1}^{N} g(\phi_j(t))\sin(\phi_j(t))\left(-k_t\sin(\phi_j(t))+k_n\cos(\phi_j(t))\right) \quad (31)$$

$$h_{yy}(t)=\sum_{j=1}^{N} g(\phi_j(t))\cos(\phi_j(t))\left(-k_t\sin(\phi_j(t))+k_n\cos(\phi_j(t))\right) \quad (32)$$

The angular position of tooth j ($\phi_j(t)$) and the function g(j(t)) are defined respectively by equations (33) and (34):

$$\phi_j(t)=(2\pi\Omega/60)t+j\,2\pi/N \quad (33)$$

where Ω is the spindle speed in (rpm).
The function g ($\phi_j(t)$) is a screen function, which is equal to one if the tooth j is in the cut, and equal to zero when the tooth j is out of the cut:

$$g(\phi_j(t))=\begin{cases}1 \text{ if } \phi_{st}<\phi_j(t)<\phi_{ex}\\ 0 \text{ otherwise}\end{cases} \quad (34)$$

where: ϕ_{st} and ϕ_{ex} are the start and exit angles of tooth j.
In the i^{th} semi discretization interval, equation (28) could be approximated as follows:

$$\begin{pmatrix}\ddot{x}(t)\\ \ddot{y}(t)\end{pmatrix}+\begin{pmatrix}2\zeta\omega_n & 0\\ 0 & 2\xi\omega_n\end{pmatrix}\begin{pmatrix}\dot{x}(t)\\ \dot{y}(t)\end{pmatrix}+\begin{pmatrix}\omega_n^2+\frac{bh_{xxi}}{m_t} & \frac{bh_{xyi}}{m_t}\\ \frac{bh_{yxi}}{m_t} & \omega_n^2+\frac{bh_{yyi}}{m_t}\end{pmatrix}\begin{pmatrix}x(t)\\ y(t)\end{pmatrix}=\begin{pmatrix}\frac{bh_{xxi}}{m_t} & \frac{bh_{xyi}}{m_t}\\ \frac{bh_{yxi}}{m_t} & \frac{bh_{yyi}}{m_t}\end{pmatrix}\begin{pmatrix}x_{\tau,i}\\ y_{\tau,i}\end{pmatrix} \quad (35)$$

By using Cauchy transformation, equation (35) could be written in the following form:

$$\dot{u}(t)=A_i u(t)+w_a B_i u_{i-m+1}+w_b B u_{i-m} \quad (36)$$

where:

$$A_i=\begin{pmatrix}0 & 0 & 1 & 0\\ 0 & 0 & 0 & 1\\ -\omega_n^2-\frac{bh_{xxi}}{mt} & -\frac{bh_{xyi}}{mt} & -2\zeta\omega_n & 0\\ -\frac{bh_{yxi}}{mt} & -\omega_n^2-\frac{bh_{yyi}}{mt} & 0 & -2\zeta\omega_n\end{pmatrix} \quad (37)$$

$$B_i=\begin{pmatrix}0 & 0 & 0 & 0\\ 0 & 0 & 0 & 0\\ \frac{bh_{xxi}}{m_t} & \frac{bh_{xyi}}{m_t} & 0 & 0\\ \frac{bh_{yxi}}{m_t} & \frac{bh_{yyi}}{m_t} & 0 & 0\end{pmatrix} \quad (38)$$

$$u(t)=\begin{pmatrix}x(t)\\ y(t)\\ \dot{x}(t)\\ \dot{y}(t)\end{pmatrix} \quad (39)$$

$$u_j=u(t_j)=\begin{pmatrix}x(t_j)\\ y(t_j)\\ \dot{x}(t_j)\\ \dot{y}(t_j)\end{pmatrix}=\begin{pmatrix}x_j\\ y_j\\ \dot{x}_j\\ \dot{y}_j\end{pmatrix} \quad (40)$$

And this new expression for $\dot{u}(t)$ is given for any integer j, with: $w_a=w_b=1/2$, since the time delay is equal to the time period.
For the initial condition $u(t_i) = u_i$, the term u_{i+1} is determined as:

$$u_{i+1}=P_i u_i+w_a R_i u_{i-m+1}+w_b R_i u_{i-m} \quad (41)$$

where:

$$p_i = \exp\left(A_i \Delta t\right) \tag{42}$$

$$R_i = \left(\exp\left(A_i \Delta t\right) - I\right) A_i^{-1} B_i \tag{43}$$

We note, that $\dot{x}\left(t-\tau\right)$ and $\dot{y}\left(t-\tau\right)$ does not appear in equation (28). Consequently, u_{i+1} depends on terms $(x_i, y_i, \dot{x}_i, \dot{y}_i, x_{i-m+1}, y_{i-m+1}, x_{i-m}, y_{i-m})$, but it does not depends on terms $(\dot{x}_{i-m+1}, \dot{y}_{i-m+1}, \dot{x}_{i-m}, \dot{y}_{i-m})$. For this, the 3rd and the 4th columns of matrices B_i and R_i are nulls. This leads to a (2m+4) dimensional state vector given as:

$$z_i = col\left(x_i \; y_i \; \dot{x}_i \; \dot{y}_i \; x_{i-1} \; y_{i-1} \ldots x_{i-m} \; y_{i-m}\right) \tag{44}$$

The resulted discrete map is given by the following expression:

$$z_{i+1} = Dz_i \tag{45}$$

where the *(2m + 4)* dimensional coefficient matrix are expressed as:

$$D_i = \begin{pmatrix} P_{i,11} & P_{i,12} & P_{i,13} & P_{i,14} & 0 & \cdots & 0 & w_a R_{i,11} & w_a R_{i,12} & w_b R_{i,11} & w_b R_{i,12} \\ P_{i,21} & P_{i,22} & P_{i,23} & P_{i,24} & 0 & \cdots & 0 & w_a R_{i,21} & w_a R_{i,22} & w_b R_{i,21} & w_b R_{i,22} \\ P_{i,31} & P_{i,32} & P_{i,33} & P_{i,34} & 0 & \cdots & 0 & w_a R_{i,31} & w_a R_{i,32} & w_b R_{i,31} & w_b R_{i,32} \\ P_{i,41} & P_{i,42} & P_{i,43} & P_{i,44} & 0 & \cdots & 0 & w_a R_{i,41} & w_a R_{i,42} & w_b R_{i,41} & w_b R_{i,42} \\ 1 & 0 & 0 & 0 & 0 & \ldots & 0 & 0 & 0 & 0 & 0 \\ 0 & 1 & 0 & 0 & 0 & \ldots & 0 & 0 & 0 & 0 & 0 \\ 0 & 0 & 0 & 0 & 1 & \cdots & 0 & 0 & 0 & 0 & 0 \\ \vdots & \vdots & \vdots & \vdots & \vdots & \ddots & \vdots & \vdots & \vdots & \vdots & \vdots \\ 0 & 0 & 0 & 0 & 0 & \cdots & 1 & 0 & 0 & 0 & 0 \\ 0 & 0 & 0 & 0 & 0 & \cdots & 0 & 1 & 0 & 0 & 0 \\ 0 & 0 & 0 & 0 & 0 & \cdots & 0 & 0 & 1 & 0 & 0 \end{pmatrix} \tag{46}$$

Here (P_i, h_j) and (R_i, h_j) are the P_i and R_i elements of the matrix respectively in h_{th} row and j column. The *(2m+4)* dimensional transition matrix Φ is determined by coupling relation (35), for $i = 0, 1, \ldots, n-1$.

$$m = \text{int}\left(\frac{\tau + \Delta t \,/\, 2}{\Delta t}\right) \tag{47}$$

The integer m could be considered as an approximation parameter regarding the time delay. The n determines the number of matrices to be multiplied in relation (48), i.e. n is the number of discretizations over one period T, with: $T = n.\Delta t$

$$\Phi = D_{n-1} D_{n-2} \cdots D_1 D_0 \tag{48}$$

If the eigenvalues of the transition matrix Φ are in modulus less than one, then the analyzed system is stable.

4. STABILITY LOBE DIAGRAMS (SLD)

In this section stability lobe diagrams presented in Figure 2 and Figure 3 are obtained by using the ZOA and SD methods, by considering the references (Altintas, 2000), (Insperger and Stépan, 2004), (Azoui and Benmohammed, 2015), and (Ramos, 2009), when using a symmetric tool (i.e. the same characteristics in X and Y directions).
A simulation program was developed by using the MATLAB software Version 7.9.0.

The stability lobe diagram is a series of scallop-shaped lobes. These lobes form the limits for chatter areas.
Locally for each lobe, there is a stable area below lobe and an unstable above the lobe (Figure 2).
As the spindle speed increases, the lobes become wider with larger intervening spaces between consecutive lobes. This phenomenon creates a desirable situation for machining at both higher speed and deeper cut simultaneously, as well as at a wider speed ranges.

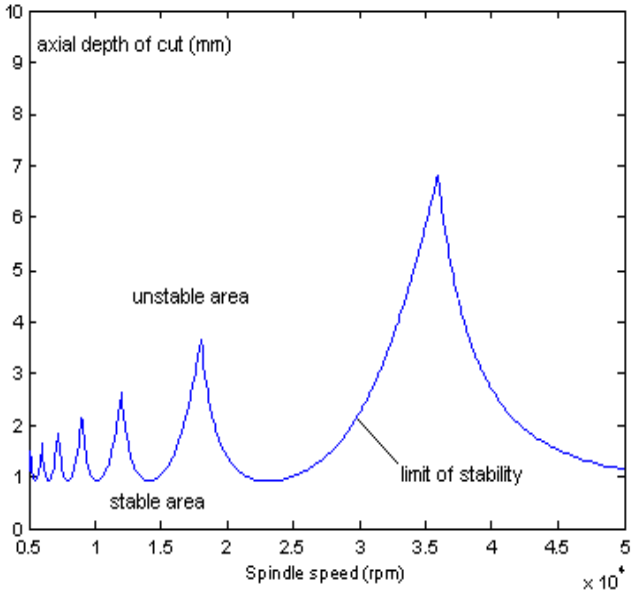

Fig. 2. Stability lobe diagram obtain.ned with ZOA method

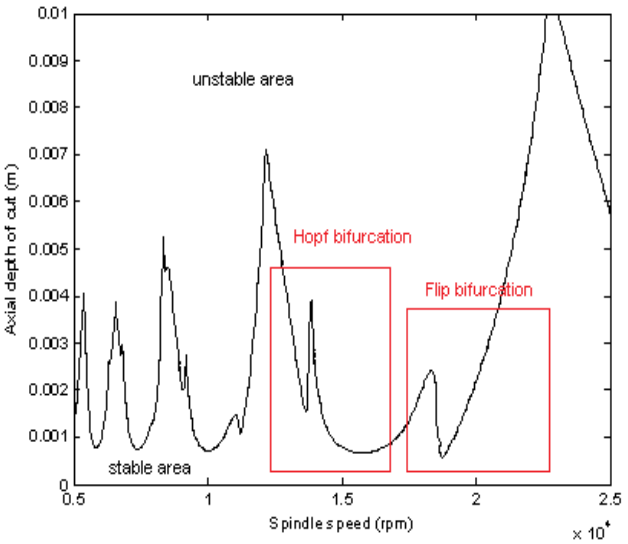

Fig. 3. Stability lobe diagram obtained with SD method

By comparing the two used methods (Figure 2 and Figure 3), we could conclude that the most significant difference is an additional set of stability lobes predicted only when using the SD method. These lobes correspond most mainly to the kind of instability called the period doubling or "flip bifurcation", which causes a periodic kind of chatter, as opposed to the quasi-periodic chatter caused by the instability, the "Hopf bifurcation".

5. CONCLUSION

The lobe stability diagrams are charts representing the stability and instability domains during machining and allow the choice of preferential cutting conditions, in order to increase machining productivity and to avoid also the machine tools vibrations.

The above two techniques ZOA and SD methods were explained and used to get the stability lobe diagrams for a 2DOF system for milling process, when using a symmetric tool having the same characteristics in the two directions X and Y. When analyzing the obtained results, it is shown that when using the SD's method, an additional set of instability appears, it is called a "flip bifurcation" and this method gives the best results.

REFERENCES

1. Altintas, Y., Budak, E., (1995). *Analytical prediction of stability lobes in milling*, Annals of the CIRP 44 (1) 357–362.

2.Altintas, Y., (2000). *Manufacturing Automation, Metal Cutting Mechanics*, Machine Tool Vibrations and CNC Design, Cambridge University Press, 298 pages.

3. Azoui, C., Benmohammed, B., (2015). *Stability Lobes for 1DOF and 2DOF Milling System*, Lecture Notes in Mechanical Engineering, Springer International Publishing Switzerland, DOI 10.1007/978-3-319-17527-0, Design and Modeling of Mechanical Systems – II, 645-650.

5. Insperger ,T., Stépan, G.,(2004). *Updated semi-discretization method for periodic delay-differential equations with discrete delay*, International journal for numerical methods in engineering, 61, 117-141.

6. Jin, G., Zhang, Q., Hao, S., Xie, Q., (2013). *Stability prediction of milling process with variable pitch cutter*, Hindawi Publishing Corporation, Mathematical Problems in Engineering, Volume Article ID 932013.

7. Khaled, S., (2013). *Modeling and analysis of chatter mitigation strategies in milling*, PhD Thesis, Department of mechanical engineering, Sheffield, UK.

8. Mlađenović, C., Zeljković, M., Košarac, A., Živković, A., (2015). *A Definition of machining systems stability lobe diagram using analytical models*, J. Prod. Eng. (JPE), 18 (1), 47-50.

9. Palpandian, P., Prabhu, R. V., Satish, B. S., (2013). *Stability lobe diagram for high speed machining processes: comparison of experimental and analytical methods – a review*, Int. J. Innov. Res. in Sci., Eng. Tech., 2(3), 747-752.

10. Paurobally, R., Siddhpura, M., (2012). *A review of chatter vibration research in turning*, Int. J. of Mach. Tools & Manu., 61, 27–47.

11. Ramos, R.E.Z., (2009). *Applying decision analysis to milling with system dynamics constraints: a new frontier in machining science*", PhD Thesis, University of Florida.

12. Landers, R.G. and Ulsoy, A.G., (1996). *Chatter analysis of machining systems with non linear force processes*, ASME International Mechanical Engineering Congress and Exposition, Atlanta, Georgia, 58, 183-190.

13. Van Ballegooijen, M.J.J., (2008). *Overview of stability analysis in machining processes*, B. Sc. (0533569), Eindhoven University of Technology, Department Mechanical Engineering, Dynamics and Control Grou, Eindhoven.

14. Wiercigroch, M., Budak, E., (2001). *Sources of non linearities, chatter generation and suppression in metal cutting*, The Royal Society, Phil. Tran. R. London, A., 359, 663-693.

Received: November 15, 2017 / Accepted: June 15, 2018 / Paper available online: June 20, 2018